Propagation velocity of pulse-like rupture along earthquake faults

Shiro Hirano

Abstract During earthquakes, the rupture front propagates along faults at approximately 40–90 % of the shear or Rayleigh wave velocity, with slip rate often concentrated in a narrow region behind the front. Past studies have considered this phenomenon using a steady-state pulse-like rupture model and a slip-weakening friction law; however, the results included a trade-off between rupture velocity and the scale of the pulse, which prevents the rupture velocity from being uniquely determined. In this study, we explore this issue and develop a model to determine rupture velocity by considering a friction law based on a numerical simulation of a past study for a slipping plane with its microscopic structure. We combine two models from past studies to construct a relationship between rupture velocity and some tectonophysical/geological parameters.

1 Introduction

Earthquakes are dynamic shear fractures along faults embedded in the Earth's crust. The spatial extension of faults covers a broad range. Small-scale faults extend $\sim$ 1mm in laboratory settings, and are equivalent to mineral grain boundaries, or $\sim$ 10cm in situ features detectable in mines. Large-scale faults extend $\sim$ 1000km along plate interfaces, and can host earthquakes of magnitude ~ 9. Geological observations have suggested that fault thicknesses are negligible with respect to fault length; therefore, regardless of scale, faulting is regarded as slip along a crack and is treated using a fracture mechanics framework in earthquake source physics

Using seismological waveform inversions under such a framework, investigations into the spatio-temporal distribution of fault rupture and slip have shown that, in some cases, entire fault surfaces do not go on slipping as the rupture propagates. Instead, the slip rate concentrates in a narrow region behind the rupture front [9].

Shiro Hirano
Ritsumeikan University, Shiga, Japan. See https://interfacial.jp/ for contact details.

This phenomenon, which is often referred to as pulse-like rupture, is distinct from crack-like rupture, during which the slip rate is sustained along the entire fault surface as the rupture extends (e.g., [9, 2, 3]).

Freund [5] theoretically simplified pulse-like rupture in 2-D by considering mode-II dynamic rupture propagation of the pulse with constant length and velocity. In his framework, the displacement field caused by the pulse was steady-state within a moving coordinate with velocity equal to that of pulse propagation. This resulted in a singular integral equation (the Airfoil equation) for slip rate inside of the pulse.

At the same time, frictional forces acting on the slipping plane are not negligible because faults are located in the Earth's crust, which is strongly compressed. Therefore, a term representing friction must be introduced in the integral equation. A simplified and classic way to model friction is to assume that constant dynamic friction works uniformly inside of a slipping region. Referred to as Coulomb's friction law, this has been accepted as an efficient approximation of friction. However, slip rates and stress near the leading edge of the pulse diverge, even though the energy release rate is finite [5]. This unphysical divergence can be removed by employing a slip-weakening friction law proposed by Ida [11] and Palmer & Rice [14]. The friction model, originally based on the results of stick-slip laboratory experiments, states that friction is a monotonically decreasing function of slip amount. The model takes a constant value equivalent to dynamic friction after the slip amount exceeds a threshold (i.e., the critical slip distance).

Using the slip-weakening friction model, Rice et al. ([15] hereinafter, RSP) provided a solution of finite slip rate; however, their solution included a trade-off between propagation velocity (rupture velocity) and the length of the pulse, meaning that these two could not be determined uniquely even after assuming values of maximum static friction, dynamic friction, initial stress acting on the fault, and surface energy. In general, rupture velocity is a significant parameter when determining kinetics on and off the fault; for example, maximum slip rate [6], stress distribution around the fault (e.g., RSP), and the dominant frequency of far-field seismic wave [4]. From an observational point of view, rupture velocity is not negligibly small, but approximately 40–90 % of the shear or Rayleigh wave velocity [7, 20]. However, because of the trade-off, even the qualitative characteristic of rupture velocity cannot be explained. For this reason, the theoretical determination of the propagation velocity of pulse-like rupture remains problematic in earthquake source physics.

In this study, we show that the lack of determinability in the RSP framework can be solved using the friction model of Hatano [8], which was developed using a numerical experiment focused on observed microscopic fault structures. We first introduce the singular integral equation for slip rate to describe the balance of traction inside of the pulse. Next, we review the theoretical model of RSP and expose the trade-off between rupture velocity and length of the pulse. After introducing the microscopic structure geologically observed in actual faults and numerically modeled by Hatano [8], we finally show that the Hatano's result contributes to solving the trade-off problem. Moreover, we consider how rupture velocity and length of the pulse depend on tectonophysical or geological parameters, and these are affected by uncertainties in the parameters.

2 Formulation

2.1 PDE and boundary conditions

We here define a 3-D coordinate, flat fault, and some physical quantities that are essentially the same as those of Freund [5] and RSP. First, as shown in Fig.1, we define domains in the x-z plane: $\Gamma = \{x,z|x \in (-\infty, v_r t), z \in \mathbb{R}\}$ and $\Gamma^* = \{x,z|x \in (v_r t - L, v_r t), z \in \mathbb{R}\} (\subset \Gamma)$, where $t \in \mathbb{R}$ is time, and v_r is the sub-sonic propagation velocity of the moving rupture front toward the positive direction of the x-axis. Physically, we regard the x-z plane as the fault, Γ as an already ruptured region, and Γ^* as a pulse (i.e., a temporarily slipping region). Next, we define the y-axis perpendicular to the x-z plane and the displacement field as $\boldsymbol{u} : \left(\mathbb{R}^3 \backslash \Gamma\right) \times \mathbb{R} \ni (x,y,z,t) \mapsto (u_x, u_y, u_z) \in \mathbb{R}^3$ due to slip on Γ. A support of the gap of displacement (i.e., slip) $[\boldsymbol{u}] := \boldsymbol{u}^+ - \boldsymbol{u}^-$ is Γ, where the superscript $\pm$ indicates $\lim_{y \to \pm 0}$. In addition, a support of the slip rate $\boldsymbol{v} := \partial_t [\boldsymbol{u}]$ is Γ^*. We assume linear elasticity for a uniform domain corresponding to $\mathbb{R}^3 \backslash \Gamma$, so our governing equation corresponds to Navier's equation:

$$
\begin{cases}
\partial_t^2 \boldsymbol{u} = c_d^2 \nabla (\nabla \cdot \boldsymbol{u}) - c_s^2 \nabla \times (\nabla \times \boldsymbol{u}) & \text{in } \mathbb{R}^3 \backslash \Gamma, \quad (1a) \\
[\boldsymbol{u}] \cdot \boldsymbol{n} = [u_y] = 0 & \text{in } \Gamma, \quad (1b) \\
(\sigma \boldsymbol{n})^+ = (\sigma \boldsymbol{n})^- & \text{in } \Gamma, \quad (1c) \\
(\sigma \boldsymbol{n})^\pm - \left\{(\sigma \boldsymbol{n})^\pm \cdot \boldsymbol{n}\right\} \boldsymbol{n} = \boldsymbol{f}(x,z,t) - \boldsymbol{T}_0(x,z) & \text{in } \Gamma^*, \quad (1d) \\
\sigma = 0 & \text{in } |x| \to \infty, |y| \to \infty, \quad (1e)
\end{cases}
$$

where c_d and c_s indicate the dilatational and shear wave velocities, respectively; note that $c_d = \sqrt{(\lambda + 2\mu)/\rho}$ and $c_s = \sqrt{\mu/\rho}$ hold, where λ and μ are the Lamé constants of rock, and ρ is the density of rock. Furthermore, $\boldsymbol{n}$ indicates a unit normal to Γ, so that eq.(1b) physically represents a non-opening (i.e., slip) condition on the fault. The tensor σ is the stress perturbation defined as

$$
\sigma := \lambda (\nabla \cdot \boldsymbol{u}) \boldsymbol{I} + \mu \left\{ \nabla \boldsymbol{u} + (\nabla \boldsymbol{u})^T \right\}, \quad (2)
$$

where $\boldsymbol{I}$ indicates the identity, so the boundary condition (1c) physically represents continuity of traction on the fault. Moreover, LHS of eq.(1d) is the shear component of traction, and $\boldsymbol{f}$ and $\boldsymbol{T}_0$ in RHS of eq.(1d) are considered to be friction and initial traction applied to Γ, respectively. We assume that $\boldsymbol{T}_0$ is uniform on Γ.

However, the PDE still lacks a boundary condition for $|z| \to \infty$ and an initial condition. Instead of assuming them explicitly, previous studies assumed a uniformity of the system along the z-axis and a steady-state. We assume that the displacement field does not depend on a position in the z-axis, which is formally equivalent to $\boldsymbol{u} = \boldsymbol{u}(x,y,t)$ and $\partial_z \boldsymbol{u} = 0$. Thus, the system no longer requires a boundary condition for $|z| \to \infty$. This assumption splits the governing equation into an in-plane problem for u_x, u_y and an anti-plane problem for u_z. Next, we assume that the displacement

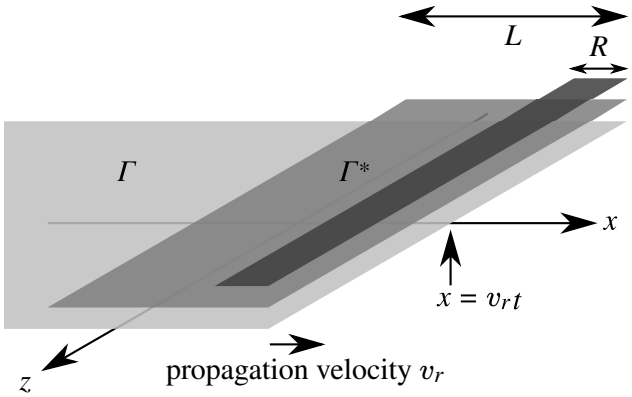

Fig. 1 Domains in the x-z plane. The light gray region indicates the ruptured region Γ, and the intermediate gray region with width L indicates the temporarily slipping region Γ^*. The dark gray region with width R indicates the process zone of slip-weakening friction defined in eq.(6). All are propagating rightward with velocity v_r.

field depends only on $(x-v_r t, y)$, as with Γ and Γ^*. This assumption allows us to apply Galilean transformation $x-v_r t \mapsto x'$ to the system, which yields $\partial_t = -v_r \partial_{x'}$. Thanks to the assumption of steady-state, we do not require an initial condition. Subsequently, we once again note x' as x; therefore, the rupture front is located at the origin of the x-y plane (i.e., $\Gamma = (-\infty, 0) \times \mathbb{R}$ and $\Gamma^* = (-L, 0) \times \mathbb{R}$).

2.2 Fundamental solution and integral equation

Regarding the representation of shear traction perturbations due to steady-state propagation of the pulse, one of the simplest cases is to apply Galilean transformation to the moving dislocation model. In the dislocation model, $[u](x) = bH(-x)$ holds when $u = u_x$ for a climbing edge dislocation (mode-II), or $u = u_z$ for a screw edge dislocation (mode-III), and where b is the magnitude of the Burgers vector, and $H(\cdot)$ is the Heaviside function. Noting $(\boldsymbol{\sigma n})^{\pm} = (T_{xy}, T_{yy}, T_{zy})^T$, these three components due to the dislocations are obtained as:

$$(T_{xy}, T_{yy}, T_{zy})^T = \frac{\mu F(v_r/c_s)}{2\pi} \frac{b}{x} \times \begin{cases} (1,0,0)^T & \text{for mode-II,} \\ (0,0,1)^T & \text{for mode-III,} \end{cases} \tag{3}$$

where

$$F(v_r/c_s) = \begin{cases} \frac{4\alpha_d \alpha_s - \left(1+\alpha_s^2\right)^2}{\alpha_s\left(1-\alpha_s^2\right)} & \text{for mode-II,} \\ \alpha_s & \text{for mode-III,} \end{cases} \tag{4}$$

and where $\alpha_d = \sqrt{1-(c_s/c_d)^2\,(v_r/c_s)^2}$, and $\alpha_s = \sqrt{1-(v_r/c_s)^2}$ (e.g., [22]). Slip rate due to the dislocation can be represented as $bv_r\delta(x)$ because $v(x) = \partial_t[u](x) = -v_r\partial_x[u](x)$ holds where $\delta(\cdot)$ is Dirac's delta function. This means that $v_r^{-1}v(x)$ is identical to the spatial distribution of b, and non-zero components in (3) can be represented as a convolution of $v_r^{-1}v(x)$ and $1/x$ for arbitrary v as:

$$T(x) = -\frac{\mu F(v_r/c_s)}{2v_r}\int_{\Gamma^*}\frac{v(\xi)}{\xi - x}\frac{d\xi}{\pi}, \tag{5}$$

where $T = T_{xy}$ for mode-II or $T = T_{zy}$ for mode-III. According to the boundary condition (1d), $(\boldsymbol{\sigma}\boldsymbol{n})^{\pm}$ is equivalent to $f(x) - T_0$ (the x component of $\boldsymbol{f} - \boldsymbol{T}_0$ for mode-II or the z component of $\boldsymbol{f} - \boldsymbol{T}_0$ for mode-III). Therefore, $T(x)$ is a function related to friction and initial traction, and $v(x)$ is an unknown function. The Airfoil equation, a singular integral equation (5), can be turned into the Riemann-Hilbert problem, and its general solution was obtained by [13].

3 Friction modeling

3.1 RSP modeling revisited

In general, a solution of eq.(5) has a square-root singularity behind the rupture front (i.e., $v(-\varepsilon) \propto 1/\sqrt{\varepsilon}$ for a sufficiently small positive value of ε). As discussed in 1, this singularity can be removed under slip-weakening friction. RSP considered $f(x)$ and $T(x)$ at $x \in \Gamma^* = (-L, 0)$ as follows:

$$T(x) + T_0 = f(x) = \begin{cases} T_s + \frac{T_s - T_d}{R}x & \text{for } -R < x \le 0, \\ T_d & \text{for } -L \le x \le -R, \end{cases} \tag{6}$$

where T_s and T_d are the maximum static friction and the dynamic friction, respectively, and should satisfy the relationship $0 \le T_d \le T_0 < T_s$. Note that eq.(6) is an actual form of eq.(1d), and the LHS of eq.(6) physically represents the total shear traction temporarily acting on the pulse. According to eq.(6), the maximum static friction occurs at the rupture front ($x = 0$), and constant dynamic friction occurs when $-L < x < -R$. Moreover, there exists a process zone for the weakening of friction at $-R < x \le 0$. Under this setting, $[u]$ increases and f decreases as x decreases in Γ^* if $v \ge 0$. Therefore, friction is a monotonically decreasing function of the slip amount. Thus, RSP considered that eq.(6) corresponds to the slip-weakening friction law.

By solving the Airfoil equation, which consists of eqs.(5) and (6), RSP obtained a condition to remove the square-root singularity as follows:

$$\frac{1}{1+S} = \frac{\theta'}{\pi} - \frac{\theta' - \sin\theta'}{2\pi\sin^2(\theta'/2)}, \tag{7}$$

where $S = (T_s - T_0)/(T_0 - T_d)$, and $\theta' = 2\arcsin\sqrt{R/L}$. This condition shows that only R/L is determined uniquely after S is given. In other words, the absolute values of L and R cannot be determined uniquely even after S is given.

RSP also considered the energy release rate due to the propagation of the pulse, which can be calculated via:

$$G = \int_0^D \{f([u]) - T_d\}\, d[u], \tag{8}$$

where $D := \lim_{t\to\infty}[u]$ is the total locked-in displacement [14]. As a result, they concluded that:

$$G = \frac{(T_s - T_d)^2 R}{\mu F(v_r/c_s)} \left(\frac{\theta'}{\pi} - \frac{\theta' - \sin\theta'}{2\pi\sin^2(\theta'/2)}\right)\left(\frac{\theta' - \sin\theta'\cos\theta'}{4\sin^4(\theta'/2)}\right). \tag{9}$$

Combining eqs.(7) and (9), we can write Ψ as a relationship between some parameters:

$$\Psi(T_s - T_d, S, G, R, v_r) = 0. \tag{10}$$

In eq.(10), a frictional parameter $T_s - T_d$, the stress ratio S and a material quantity G can be regarded as prescribed mechanical parameters independent of kinematics. On the other hand, R and v_r are kinematic parameters that describe an apparent movement of the system. Hence, in view of mechanics, R and v_r are determined after the mechanical parameters are given. However, eq.(10) means that there exists a trade-off between R and v_r, which cannot be determined uniquely on the basis of this single relationship. Therefore, another relationship between R and v_r needs to be identified.

3.2 Modeling the microscopic structure of fault planes

During modeling, prior studies neglected fault thickness; although, geologists have observed small but finite thicknesses of localized shear layers in fault outcrops. These layers are full of a finely crushed matrix (or fault gouge) and have thicknesses of 10^{-4}m to 10^{2}m, roughly proportional to 10^{-4} times fault length (e.g., [16, 18]). Therefore, the regions Γ and Γ^* in our notation are extended to $\Gamma = \{x, y, z | x < 0, y \in B, z \in \mathbb{R}\}$ and $\Gamma^* = \{x, y, z | x \in (-L, 0), y \in B, z \in \mathbb{R}\}$, respectively, where $B := (-H_0/2, +H_0/2)$, and a small constant H_0 is the thickness of the gouge layer. The fault gouge likely plays a significant role in the energy dissipation processes of faulting. Hatano [8] modeled each particle of a granular layer as an elastic sphere and numerically simulated the macroscopic frictional behavior of the gouge

layer using a discrete element method. In his model, the granular layer was sandwiched between two rigid walls, one of which was forced to slide at a given rate. When the rate was changed in a step-like manner, frictional resistance between the granular layer and the wall varied continuously; on this basis, Hatano [8] obtained a relaxation time τ for the transient variation, which was independent of the slip rate and was given as:

$$\tau = cH_0\sqrt{\frac{\rho_p}{P}}, \tag{11}$$

where $c \sim 1.0$ is a numerical constant, ρ_p is density of the particle, and P is pressure acting on the layer. This means that the relaxation time of friction is prescribed prior to slippage. Moreover, Hatano [8] suggested that τ can roughly represent the scale of transient time from the maximum static friction to dynamic friction. Therefore, these findings presented the possibility for a model of rupture propagation that incorporated the weakening process of friction.

3.3 Determination of kinematic parameters

As discussed, our x was originally $x - v_r t$ before the Galilean transformation was applied, while the relaxation time is eq.(11) if the slipping plane consists of a granular layer. By returning x into $x - v_r t$ and considering eq.(6), we find that the slip-weakening friction assumed by RSP has a relaxation time of R/v_r. Hence,

$$\tau = \frac{R}{v_r} \tag{12}$$

can be regarded as a constant. It is clear that eq.(12) represents another trade-off between R and v_r; therefore, the two parameters are uniquely determined after substituting eq.(12) into (10). Moreover, by taking eq.(11) into account, we obtain a relationship between the parameters $T_s - T_d, S, G, H_0, \rho_p, P$, and v_r. Furthermore, considering eqs.(5), (7) and (12), we are also able to uniquely determine slip rate $v(x)$, slip $[u](x) = -v_r^{-1}\int_0^x v(\xi)d\xi$, and pulse length L.

4 Discussion

4.1 Analysis with huge uncertainties of parameters

In general, the tectonophysical and geological parameters T_s, T_d, T_0, G, H_0 and P contain huge uncertainties, of which we often know only the order. Therefore, we propose only a rough determination of kinematic parameters (e.g., v_r, R and L) de-

pending on the order. By defining $R_0 := \lim_{v_r \to 0} R$ and regarding eqs.(9), RSP obtained the following:

$$\frac{R}{R_0} = \frac{F(v_r/c_s)}{F(0)}. \tag{13}$$

On the other hand, eq.(12) is equivalent to the following:

$$\frac{R}{R_0} = \frac{\tau c_s}{R_0} \frac{v_r}{c_s}. \tag{14}$$

Fig.2 shows a curve and line based on eqs.(13) and (14), respectively, where their intersection provides actual values of v_r/c_s and R/R_0. The slope of the line, which corresponds to the coefficient $\tau c_s/R_0$ in eq.(14), depends on the aforementioned uncertain parameters, while eq.(13) depends only on v_r/c_s. Therefore, we are only able to consider the order of the coefficient. With respect to Fig.2, we make the rough divisions:

$$\begin{cases} v_r/c_{\mathrm{lim}} \ll 1 & \text{if } \tau c_s/R_0 \gg 1, \\ v_r/c_{\mathrm{lim}} \sim 0.7 & \text{if } \tau c_s/R_0 \sim 1, \\ v_r/c_{\mathrm{lim}} \sim 1 & \text{if } \tau c_s/R_0 \ll 1, \end{cases} \tag{15}$$

where c_{lim} is the Rayleigh wave velocity for mode-II, or the shear wave velocity for mode-III. As discussed in 1, v_r/c_{lim} is usually approximately 40–90 %. Hence, we conclude that: 1) rupture velocity of several tens of percent for c_{lim} is possible when $\tau c_s/R_0$ is near unity; 2) rupture velocity approximately equivalent to c_{lim} is possible when $\tau c_s/R_0$ is negligible; and 3) slow rupture velocity is rarely observed, likely because $\tau c_s/R_0$ is not sufficiently greater than unity.

4.2 Applicability to interfacial problem

Faults commonly lie along material interfaces (e.g., plate boundaries and other tectonic lines), and the theoretical modeling discussed in 2 and 3.1 has been extended to such interfacial problems [21, 1, 10]. Especially, in the case of mode-II, normal stress perturbation inside of an interfacial pulse, the second component of eq.(3), is not zero, but rather is Dirac's delta function with the sign dependent on the direction of rupture propagation [21]. Hence, many studies have predicted asymmetric or unidirectional rupture along material interfaces, while others have actually observed [17, 12]; however, a theoretical understanding of them is still needed.

Hirano & Yamashita [10] extended the method of RSP and derived a Carleman-type singular integral equation (c.f., [19]) instead of eq.(5). On solving the equation, they found a relationship between some parameters (i.e., generalization of eqs.(7)), which removed divergence of the slip rate near the leading edge of an interfacial pulse. This generalized relationship included not only S and R/L, but also the direc-

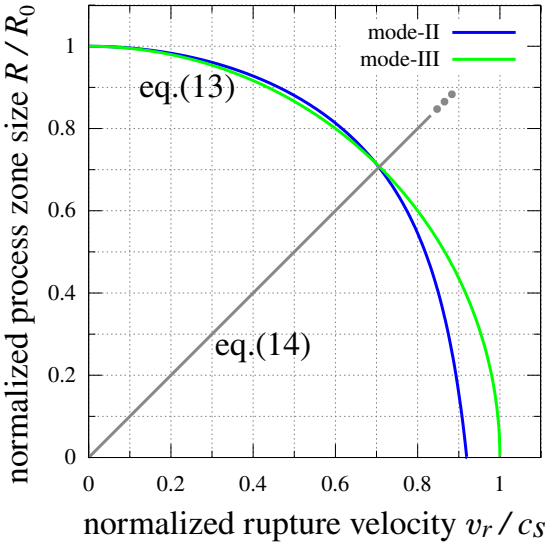

Fig. 2 Plot of eq.(13), where blue denotes mode-II and green denotes mode-III, and eq.(14). For mode-II, $c_d/c_s = \sqrt{3}$ is assumed, which is equivalent to Poisson's ratio of $1/4$ and an approximate value for crustal rocks. Zero of the curve for mode-II is identical to the Rayleigh wave velocity.

tion and velocity of pulse propagation. Moreover, G for the interfacial pulse can be determined by using their solution for slip rate and eq.(8). Therefore, we can now extend eq.(10) and our modeling to determine propagation velocity of the interfacial pulse, which can be asymmetric or unilateral.

5 Conclusions

We reviewed the methods of RSP for modeling the propagation of the pulse-like rupture with the slip-weakening friction law and highlighted their difficulties in the determination of the propagation velocity of pulse-like rupture. Considering the frictional model of Hatano [8], we proposed determinability of the propagation velocity. The propagation velocity depends on some tectonophysical/geological parameters, which usually have huge uncertainty, and we discussed the velocity only on the basis of orders of the parameters. Even with such uncertainty, we found that we could roughly estimate the propagation velocity and discuss why propagation velocity is not negligibly low. Moreover, we showed that our method can be extended to a problem of interfacial rupture propagation, which is important and controversial in earthquake source physics.

Acknowledgement

The author is grateful to T. Yamashita and T. Hatano for helpful discussions. This is a post-peer-review, pre-copyedit version of an article published in Itou, H. *et al*. (eds) *Mathematical Analysis of Continuum Mechanics and Industrial Applications. CoMFoS15*. Mathematics for Industry, Springer. The final authenticated version is available online at: https://doi.org/10.1007/978-981-10-2633-1_10.

References

1. Adda-Bedia, M. & Ben Amar, M.: Self-sustained slip pulses of finite size between dissimilar materials, J. Mech. Phys. Solids, **51**, 1849–1861 (2003)
2. Ampuero, J.-P. & Ben-Zion, Y.: Cracks, pulses and macroscopic asymmetry of dynamic rupture on a bimaterial interface with velocity-weakening friction, Geophys. J. Int., **173**, 674–692 (2008)
3. Bizzarri, A.: On the deterministic description of earthquakes, Rev. Geophys., **49**, RG3002 (2011)
4. Dong, G. & Papageorgiou, A.S.: Seismic Radiation from a Unidirectional Asymmetrical Circular Crack Model, Part I: Constant Rupture Velocity, Bull. Seism. Soc. Am., **92**(3) 945–961 (2002)
5. Freund, L.B.: Dynamic Fracture Mechanics, Cambridge Univ. Press, New York (1990)
6. Gabriel, A.-A., Ampuero, J.-P., Dalguer, L.A. & Mai, P.M.: Source properties of dynamic rupture pulses with off-fault plasticity, J. Geophys. Res. Solid Earth, **118**, 4117–4126 (2013)
7. Geller, R.J.: Scaling relations for earthquake source parameters and magnitudes, Bull. Seism. Soc. Am., **66**(6) 1501–1523 (1976)
8. Hatano, T.: Scaling of the critical slip distance in granular layers, Geophys. Res. Lett., **36**, L18304 (2009)
9. Heaton. T.H.: Evidence for and implications of self-healing pulses of slip in earthquake rupture, Phys. Earth Planet. Int., **64**, 1–20 (1990)
10. Hirano, S., & Yamashita, T.: Modeling of interfacial dynamic slip pulses with slip-weakening friction, under review
11. Ida, Y.: Cohesive force across the tip of a longitudinal shear crack and Griffith 's crack specific surface energy, J. Geophys. Res. **77**, 3796–3805 (1972)
12. Kane, D.L., Shearer, P.M., Goertz-Allman, B.P., & Vernon, F.L.: Rupture directivity of small earthquakes at Parkfield, J. Geophys. Res., **118**, 1–10 (2013)
13. Muskhelishvili, N.I.: Singular Integral Equations, Groningen, P .Noordhoff Ltd. (1953)
14. Palmer, A.C., & Rice, J.R.: The growth of slip surfaces in the progressive failure of overconsolidated clay, Proc. R. Soc. London, A **322**, 527–548 (1973)
15. Rice, J.R., Sammis, C.G., & Parsons, R.: Off-fault secondary failure induced by a dynamic slip pulse, Bull. Seism. Soc. Am., **95**(1) 109–134 (2005)
16. Robertson, E.C.: Continuous formation of gouge and breccia during fault displacement, in Issues in Rock Mechanics, Proc. Symp. Rock Mech. 23rd, eds. R. E. Goodman and F. Hulse. New York, New York: Am. Inst. Min. Eng., pp. 397–404 (1982)
17. Rubin, A. & Gillard, D.: Aftershock asymmetry/rupture directivity among central San Andreas fault microearthquakes, J. Geophys. Res., **105**, 19,095–19,109 (2000)
18. Scholz, C.H.: Wear and gouge formation in brittle faulting, Geology, **15**, 493–495 (1987)
19. Tricomi, F.G.: Integral equations, New York: Dover (1957)
20. Venkataraman, A. & Kanamori, H.: Observational constraints on the fracture energy of subduction zone earthquakes, J. Geophys. Res., **109**, B05302 (2004)

21. Weertman, J.: Unstable slippage across a fault that separates elastic media of different elastic constants, J. Geophys. Res., **85**, 1455–1461 (1980)
22. Weertman, J., and Weertman, J.R.: Moving dislocations, in Dislocations in Solids, vol. 3, chap. 8, edited by F. R. N. Nabarro, pp. 1–59, North-Holland Publ. Co., Amsterdam (1980)